Separation Science and Technology
Publication details, including instructions for authors and subscription information:
http://www.informaworld.com/smpp/title~content=t713708471

Displacement and Dispersion of Particles of Finite Size in Flow Channels with Lateral Forces. Field-Flow Fractionation and Hydrodynamic Chromatography

J. Calvin Giddings[a]
[a] DEPARTMENT OF CHEMISTRY, UNIVERSITY OF UTAH, SALT LAKE CITY, UTAH

To cite this Article Giddings, J. Calvin(1978) 'Displacement and Dispersion of Particles of Finite Size in Flow Channels with Lateral Forces. Field-Flow Fractionation and Hydrodynamic Chromatography', Separation Science and Technology, 13: 3, 241 — 254

To link to this Article: DOI: 10.1080/01496397808060222

URL: http://dx.doi.org/10.1080/01496397808060222

SEPARATION SCIENCE AND TECHNOLOGY, 13(3), pp. 241–254, 1978

Displacement and Dispersion of Particles of Finite Size in Flow Channels with Lateral Forces. Field-Flow Fractionation and Hydrodynamic Chromatography

J. CALVIN GIDDINGS

DEPARTMENT OF CHEMISTRY
UNIVERSITY OF UTAH
SALT LAKE CITY, UTAH 84112

Abstract

The role of finite particle size is established for two flow-channel separation techniques: hydrodynamic chromatography (HC) and field-flow fractionation (FFF). Both mean displacement velocity and dispersion are affected. A model is established where, for simple channel symmetries, the influence of particle size is calculated in terms of modifications of the known FFF equations for infinitely small particles displaced in a narrow channel and subject to lateral forces. This approach avoids the tedium of obtaining new solutions to the basic mass-transport equations, and the results automatically relate to those at the zero-size limit. Specific equations are derived for channels between infinite parallel walls. The retention ratio is treated first; this parameter yields the mean displacement velocity. The plate height, which is treated subsequently, yields effective axial dispersion. Plots of the relevant equations are given and some implications and complications in the theory of HC and FFF are noted.

INTRODUCTION

The behavior of particles of finite size in flow channels not enormously larger in size has drawn attention recently because of its importance in certain natural phenomena and in particle fractionation methodology. As an example of the former, the displacement of red blood cells through the fine capillaries of the extrema of the circulatory system show strong particle size effects (*1*).

A finite particle/channel size ratio is responsible for fractionation in the technique known as hydrodynamic chromatography, or separation by flow (*2–6*). In this technique, advantage is taken of the fact that the center of mass of the particle is unable to approach the wall within a distance less than one effective particle radius. Large particles as a whole are thus forced more than small particles into the center of the flow channel where displacement velocity is highest. A size-based fractionation results.

Field-flow fractionation (FFF) is another method that usually separates particles on the basis of size or mass (*7–13*). In this case larger particles are forced preferentially toward the wall. This is a result of lateral forces which interact most strongly with the largest particles, or of a reduced diffusional flux of the largest particles away from the wall once driven there by the forces. The forces, or more properly the *effective forces*, used for this purpose are thermal gradients (*9*), sedimentation forces (*10, 11*), electrical forces (*14*), and lateral flow displacements (*12*). Clearly, when solute particles are large enough that their diameters become a significant fraction of the mean thickness l of the solute cloud or of the width w of the channel, retention and plate height (zone dispersion) parameters are perturbed by the inability of the particle center of gravity to reach the walls.

The paper preceding this, by Gaydos and Brenner, provides a fundamental treatment of this problem. It includes the theory of nonspherical particles. This theory is an outgrowth of earlier work by these authors which includes finite size effects but not effective force effects (*15*).

Our approach represents a different line of attack. We simplify it by assuming that the particles can be treated as rigid spheres of radius a; that particle diffusivity is everywhere described by a single constant, D; that the flow is Newtonian and laminar; and that the particle velocity induced by flow is equal to the unperturbed stream velocity at the position of the center of mass.

With these assumptions, mean solute velocity (retention) and zone dispersion (plate height) in certain symmetrical channels can be written in terms of the known equations applicable to particles of infinitesimal size. This fact is particularly useful in the case of dispersion theory because the equations of dispersion in the presence of a lateral field are unusually complicated (*16–18*). Not only is repetition of the tedious derivation for particles of finite size avoided, but also the variations caused by increasing particle size emerge directly as a result of the nature of the approach.

It the present model the finite size of the solute particle excludes its center of gravity from a layer of thickness a adjacent to the wall. In the case of a channel of circular cross section, or one bounded by two infinite parallel

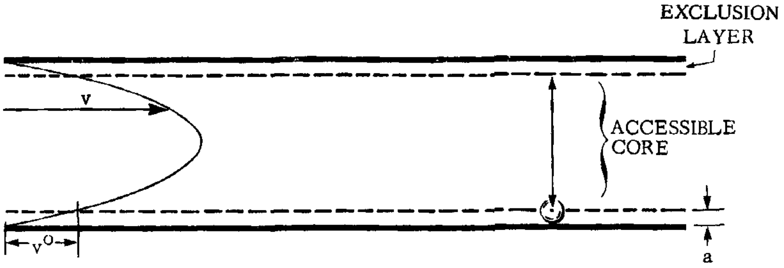

FIG. 1. Spherical particle in flow channel subject to a lateral force. The particle's center of gravity, unable to approach closer than distance *a* to the wall, executes Brownian displacements only in the "accessible core."

planes, the center of gravity executes Brownian translation over a reduced cross-sectional area, but the accessible cross section maintains its original symmetry. This can be seen by reference to Fig. 1. We term the reduced area available to the particle's center as the *accessible core*, or simply the *core*, and the inaccessible region next to the wall as the *exclusion layer*.

Under laminar conditions, flow in the core is described by the same parabolic equations that describe flow over the entire channel cross section. Thus the core becomes, for all practical purposes, a flow channel in its own right, with the same symmetry and flow characteristics as possessed by the parent channel. Hence the theory of the latter, which is well developed, can be applied to the core and the spheres diffusing therein.

Below we apply this concept to flow in narrow channels between parallel plates, but the same arguments can be applied to channels of circular cross section. We allow for the existence of a lateral field perpendicular to the faces of the plates, capable of displacing solute species in a way characteristic of field-flow fractionation methodology.

We designate by the use of the superscript, (*), each of the quantities related to core flow. All such variables will be formulated in such a manner that the core will appear as a closed flow tube with stationary walls. These effective walls will, of course, be traveling at velocity v^0 relative to the real walls confining the parent channel (see Fig. 1). Quantities related to the parent channel—and thus to the laboratory frame of reference—are those without superscript (*).

Flow velocity v as a function of distance x from the wall of the parent channel is given by the usual parabolic expression

$$v = 6\langle v\rangle\left(\frac{x}{w} - \frac{x^2}{w^2}\right) \tag{1}$$

The velocity, v^0, at the core boundary is found by substituting particle radius a for x in this expression. We get

$$v^0 = 6\langle v\rangle(\alpha - \alpha^2), \qquad \frac{1}{2} \geq \alpha \geq 0 \tag{2}$$

where $\alpha = a/w$.

We now introduce some core parameters. Mean core flow velocity $\langle v^*\rangle$ is written as

$$\langle v^*\rangle = \frac{1}{w - 2a}\int_a^{w-a} (v - v^0)\,dx \tag{3}$$

where v^0 is substracted because core quantities are defined as those resulting when the core boundary is considered stationary. The substitution of Eqs. (1) and (2) into (3), followed by integration and simplification, yields

$$\frac{\langle v^*\rangle}{\langle v\rangle} = (1 - 2\alpha)^2 \tag{4}$$

which, of course, approaches unity as $\alpha \to 0$.

MEAN DISPLACEMENT VELOCITY

The mean velocity of solute in the laboratory (parent channel) coordinate system is simply

$$\mathscr{V} = v^0 + R^*\langle v^*\rangle \tag{5}$$

where R^* is the retention ratio (solute velocity/mean solvent velocity) for the inner core. [Quantity R^* can be made <1 by the application of external fields; this is done routinely to achieve selective retention and thus separation in field-flow fractionation (*7–14*).]

The retention ratio for the parent channel—which is the observed retention ratio—is

$$R = \frac{\mathscr{V}}{v} = \frac{v^0 + R^*\langle v^*\rangle}{\langle v\rangle} \tag{6}$$

When Eqs. (2) and (4) are substituted into this, we obtain

$$R = 6(\alpha - \alpha^2) + R^*(1 - 2\alpha)^2 \tag{7}$$

It is useful now to define another retention ratio, R_{id}. This is the hypothetical value calculated on the assumption that the particle center can reach the channel wall. We refer to this assumed condition as *ideal*; in FFF this condition is part of a broader definition of ideality.

Quantity R_{id} (along with the other R parameters) can be expressed in terms of a more fundamental parameter, λ_{id}. The theory of FFF yields (*8*)

$$R_{id} = 6\lambda_{id}[\coth(1/2\lambda_{id} - 2\lambda_{id}] \tag{8}$$

Parameter λ relates directly to the force or effective force, F, by means of which the field impels the particle toward one wall of the channel. We have (*8*, *10*)

$$\lambda_{id} = kT/Fw \tag{9}$$

where k is Boltzmann's constant and T is the absolute temperature. Alternatively, F can be replaced by Uf and kT by Df to yield (*8*)

$$\lambda_{id} = D/Uw \tag{10}$$

where U is the drift velocity induced by the field, D is the particle diffusion coefficient, and f the friction coefficient.

When finite particle diameter is accounted for, channel width w must be replaced by core width $w - 2a = w(1 - 2\alpha)$, and we have

$$\lambda^* = \lambda_{id}/(1 - 2\alpha) \tag{11}$$

The core retention ratio is related to this by the same fundamental theoretical expression used in Eq. (8):

$$R^* = 6\lambda^*\{\coth(1/2\lambda^*) - 2\lambda^*\} \tag{12}$$

By combining Eqs. (7), (11), and (12), we obtain for the observed retention ratio R:

$$R = 6(\alpha - \alpha^2) + 6\lambda_{id}(1 - 2\alpha)\left\{\coth\left(\frac{1 - 2\alpha}{2\lambda_{id}}\right) - \frac{2\lambda_{id}}{1 - 2\alpha}\right\} \tag{13}$$

Several limiting forms have special applications. Hydrodynamic chromatography is realized in the absence of a lateral force, a condition for which λ_{id} approaches ∞. Under these conditions

$$\begin{aligned} R &= (1 - 6\alpha^2 + 4\alpha^3)/(1 - 2\alpha) \\ \lambda_{id} &\to \infty \end{aligned} \tag{14}$$

For field-flow fractionation, α and λ are typically small, yielding the following expression for R when expanded around zero:

$$R = 6\alpha + 6\lambda_{id} - 6\alpha^2 - 12\lambda_{id}\alpha - 12\lambda_{id}^2 + \cdots \tag{15}$$

An approximation valid for very small α's and λ_{id}'s is therefore

$$R = 6\alpha + 6\lambda_{id} \tag{16}$$

Values of R from Eq. (13) are plotted as a function of α for various λ_{id} values in Fig. 3. The values shown for $\alpha \rightarrow 0.5$ will, of course, be in significant error because the assumption that the particle travels at the unperturbed flow velocity at its center is clearly inappropriate as the particle approaches a size that spans the entire channel. As expected, increasing particle size (increasing α) causes an increase in R because the particles are forced deeper into the high flow region near the channel center.

The increase in migration rate with increasing α is the phenomenon underlying fractionation in hydrodynamic chromatography (*2–6*). The appropriate curve is the upper one, $\lambda_{id} = \infty$, in Fig. 3. The fact that solute always advances more rapidly than solvent in this system is manifested by $R \geq 1$. The fractionation sequence is such that large particles are eluted before small particles.

By contrast, in field-flow fractionation finite particle size causes no more than a perturbation on the basic fractionation effect induced by the applied field. The perturbation, however, is generally counterproductive because the normal elution sequence is such that the largest particles arrive last. The convergence of the lines in Fig. 3 with increasing α is one illustration of this, as can be seen by noting that the increments between lines is proportional to relative velocity differences. More important—and not at all obvious from the plots because they represent constant λ_{id} values—is the perturbation as α and λ_{id} both approach zero. This is described by Eq. (16). As particle size increases, the λ_{id} term of this equation always decreases in FFF, and the α term increases. At a critical diameter the effects will exactly balance one another, and there will be no size discrimination—that is, no size-based separation occurs. For example, in flow FFF in which λ_{id} is inversely proportional to a, size discrimination will disappear when $\alpha = \lambda_{id}$ or $a = w\lambda_{id}$. As particle radius increases beyond this, the larger particles will begin emerging earlier, contrary to the normal trend in FFF. In the case of sedimentation FFF, size discrimination will disappear at $a = 3w\lambda_{id}$, as a consequence of the fact that λ_{id} is inversely proportional to a^3.

PEAK DISPERSION

The theory of peak dispersion proceeds similarly. In the case where particles are assumed *not* to be excluded from the wall region, the plate height assumes it ideal form

$$H_{id} = \chi_{id} w^2 \langle v \rangle / D \tag{17}$$

where χ_{id} is a dimensionless coefficient that varies in a complicated way with λ_{id}. It is represented by $\chi_{id} = \chi(\lambda_{id})$. An explicit expression for $\chi(x)$ is given elsewhere (*17*). The present approach avoids the necessity for a separate derivation of a "χ" term in order to incorporate particle size effects.

The above equation can be readily modified to represent the core plate height

$$H^* = \chi^*(w - 2a)^2 \langle v^* \rangle / D \tag{18}$$

where $\chi^* = \chi(\lambda^*)$.

The term *plate height*—used frequently as a dispersion parameter (*19*)—can be defined as $2x$ (effective dispersion coefficient)/(mean displacement velocity). It is equivalent to the distance-based rate of generation of variance, σ^2, in the peak width; thus the core plate height becomes

$$H^* = d\sigma^2 / dZ^* \tag{19}$$

whereas the plate height of the parent channel (the experimental quantity) is

$$H = d\sigma^2 / dZ \tag{20}$$

where Z^* and Z are the mean distances of displacement of the solute in the core and the parent channel, respectively. The two coordinate systems are illustrated in Fig. 2.

One can obtain the observed plate height value defined by Eq. (20) from the theoretically calculable value of Eq. (19) by using dZ^*/dZ as a multiplying factor. This factor is simply the ratio of velocities, $(dZ^*/dt)/dZ/dt$, or $R^*\langle v^* \rangle / R\langle v \rangle$. Using this fact and Eq. (6) to obtain the latter ratio, we have

$$H = H^*(1 - v^0 / R\langle v \rangle) \tag{21}$$

When combined with Eq. (18) this yields

$$H = \chi^* \frac{(w - 2a)^2 \langle v^* \rangle}{D} (1 - v^0 / R\langle v \rangle) \tag{22}$$

Upon using $\alpha = a/w$ along with Eqs. (2), (4), (6), and (7), we obtain

$$H = \frac{\chi^* w^2 \langle v \rangle}{D} \left[\frac{R^*(1 - 2\alpha)^6}{6(\alpha - \alpha^2) + R^*(1 - 2\alpha)^2} \right] \tag{23}$$

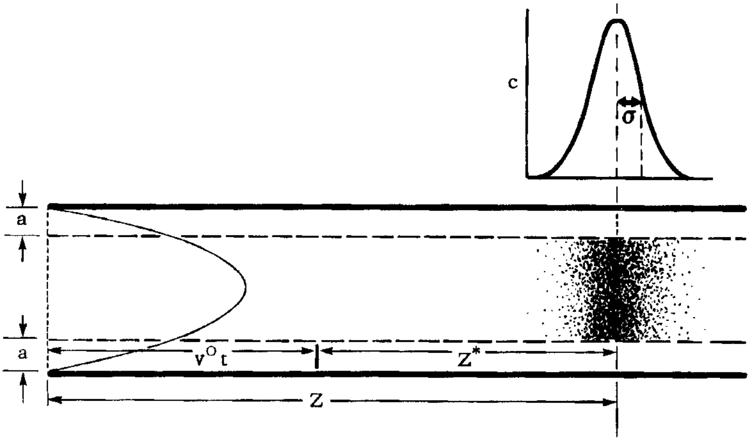

FIG. 2. Coordinate system for measuring peak dispersion in terms of plate height using Eqs. (19) and (20).

In view of the similar form of this and Eq. (17), the ratio of H to its ideal value is

$$\frac{H}{H_{id}} = \frac{\chi^*}{\chi_{id}}\left[\frac{R^*(1 - 2)^6}{6(\alpha - \alpha^2) + R^*(1 - 2\alpha)^2}\right] \tag{24}$$

When χ^* and χ_{id} are written as $\chi(\lambda^*)$ and $\chi(\lambda_{id})$, respectively, and Eq. (11) is used for λ^*, we get

$$\frac{H}{H_{id}} = \frac{\chi(\lambda_{id}/(1 - 2\alpha))}{\chi(\lambda_{id})}\left[\frac{R^*(1 - 2\alpha)^6}{6(\alpha - \alpha^2) + R^*(1 - 2\alpha)^2}\right] \tag{25}$$

When λ^* from Eq. (11) is substituted into Eq. (12), and the latter used for R^* in Eq. (25), we get

$$\frac{H}{H_{id}} = \frac{\chi(\lambda_{id}/(1 - 2\alpha))}{\chi(\lambda_{id})}\left[\frac{(1 - 2\alpha)^2}{\dfrac{(\alpha - \alpha^2) + (1 - 2\alpha)}{\lambda_{id}\left\{\coth\left(\dfrac{1 - 2\alpha}{2_{id}}\right) - \dfrac{2\lambda_{id}}{1 - 2\alpha}\right\}}}\right] \tag{26}$$

In the limit applicable to hydrodynamic chromatography, $\lambda_{id} = \infty$, this equation reduces to

$$\frac{H}{H_{id}} = \left[\frac{(1 - 2\alpha)^3}{6(\alpha - \alpha^2) + (1 - 2\alpha)^2}\right] \tag{27}$$

and when α and λ_{id} both approach zero

$$\frac{H}{H_{id}} = \frac{\lambda_{id}}{\alpha + \lambda_{id}} \tag{28}$$

a limit reasonably descriptive of practical FFF.

Equation (26) is explicit in α and λ_{id} except in the χ functions. For the latter, an explicit expression has been reported elsewhere (*17*). Using this source the ratio of χ functions, $\chi(\lambda_{id}/(1 - 2\alpha))/\chi(\lambda_{id})$, has been evaluated for various λ_{id}'s and α's. This ratio has been combined with the remainder of Eq. (26) and plotted in Fig. 4 as the H/H_{id} ratio. Clearly, finite particle size is associated with a reduction in plate height relative to the zero-size limit.

DISCUSSION

In Figs. 3 and 4, hydrodynamic chromatography (HC) corresponds to the single curve representing the absence of external forces: $\lambda_{id} = \infty$. These solutions by themselves are not unusually significant, for two reasons. First, a more comprehensive analysis for this special case has been given in the literature (*2, 3*). The equations—like those presented here—are valid for tubes of perfectly uniform cross section.

Second, if randomly packed beds are used for HC, the flow channels cannot be represented by a parallel series of uniform tubes or slits. Analogous attempts in other forms of chromatography have largely failed (*19*), and they are expected to do so even more in HC because of more sluggish diffusion. To account for experimental observations in chromatography, it is necessary to allow for the dispersion due to the random flow pattern. When calculated for liquid chromatography, this effect is much smaller than the dispersion accounted for here. Unfortunately, for the simple theories, the effects are not additive. More detailed considerations show that these two effects are combined in approximate accord with the *coupling equation* (*19–23*)

$$H = 1 \Bigg/ \left(\frac{1}{H_N} + \frac{1}{H_F}\right) \tag{29}$$

where H_N is the nonequilibrium plate height term—the subject of the main theoretical treatment of this paper—and H_F is the contribution of random flow in the absence of diffusion. Because quantity H_N is inversely proportional to particle diffusivity, it is relatively large in all forms of liquid chromatography, usually to such a degree that $H_N \gg H_F$. Under these

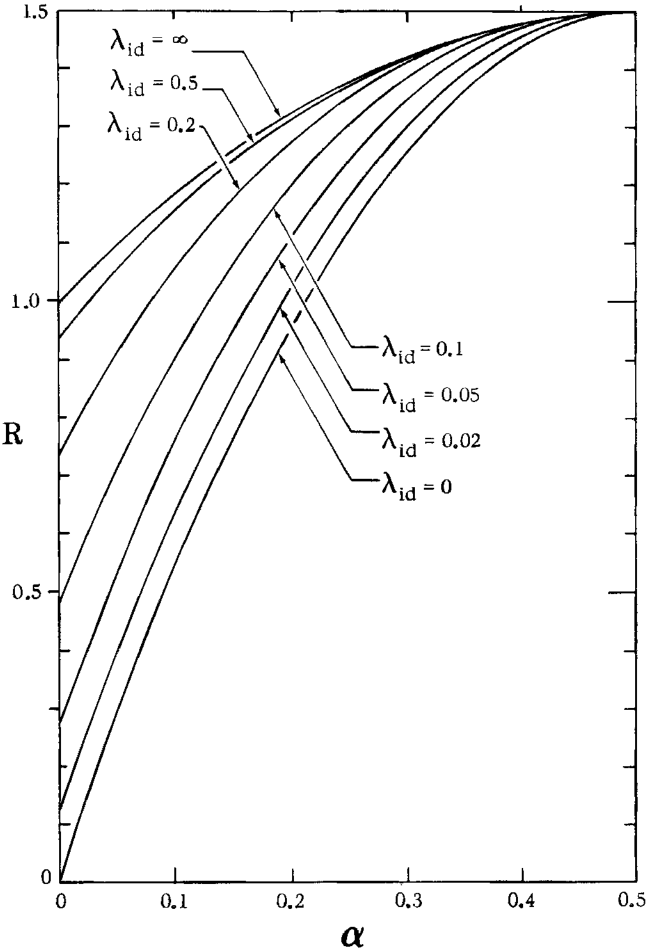

FIG. 3. Variation of retention ratio R with the ratio, α, of particle radius to channel width at various values of λ_{id}. Equation (13) was used for this plot.

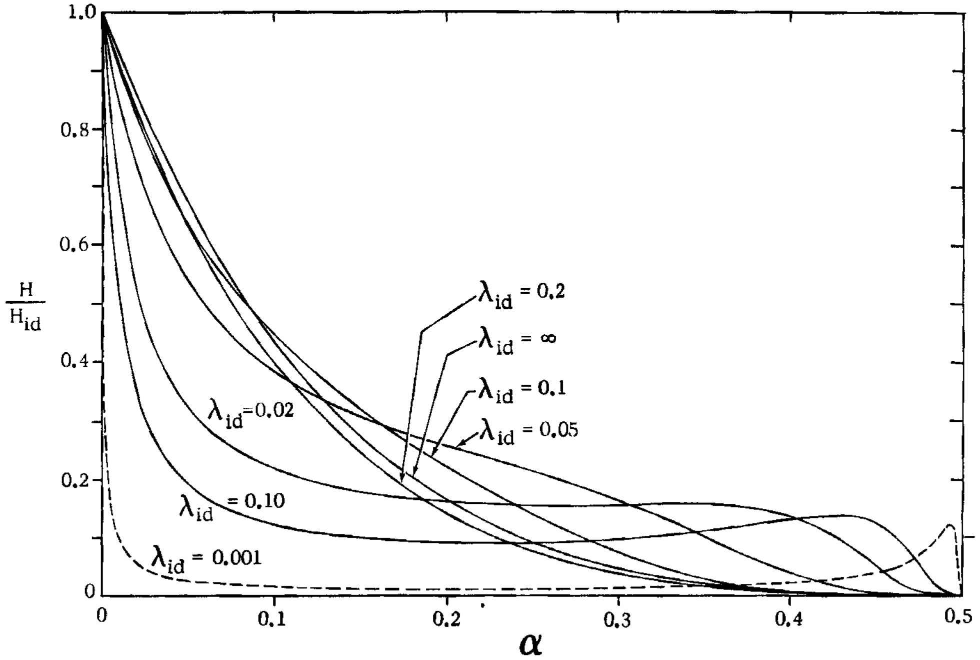

FIG. 4. Ratio of plate height, H, to its value (ideal) in the absence of particle-size effects, H_{id}, as a function of dimensionless particle size, α.

circumstances its influence largely disappears, and Eq. (29) yields

$$H \sim H_F = \text{const} \times d_p \qquad (30)$$

an equation showing that H approaches H_F, a constant for a given chromatographic bed packed with particles of mean diameter d_p. The approximate order of magnitude of the various terms given here is provided elsewhere (*19*).

Random beds may also complicate mean displacement velocities in HC. Because of the large size of the solute particles, they will be carried repeatedly against the walls of the fixed particles as flow channels split around obstacles and the streamlines graze within distance a of various elements of solid surfaces. Once forced against the surface, their progress would be slowed or halted. Their progress would not fully resume until the particles were "rolled" along and finally away from the surfaces by flow, or until they escaped by diffusion. The larger particles, having more sluggish diffusion, would tend to become trapped in crevices and aperatures through which the fluid could pass, but they could not. Escape would be likely only in cases where a very small diffusional displacement would free the particle. The effective mean back-diffusional distance against a flow stream of velocity v is $l = D/U$ (*12*), which may typically be as small as $(10^{-8}\ \text{cm}^2/\text{sec})/(10^{-2}\ \text{cm/sec}) = 10^{-6}$ cm. This is many times smaller than the diameter of some particles of interest. Diffusional fluctuations would somewhat enlarge the effective escape path calculated here, but not to a major degree.

In short, one would expect a retardation and trapping effect not accounted for in the simple theory. The effect would increase with particle diameter and flow velocity.

The retardation effect might best be accounted for by a simple model of electrophoretic migration (*24*). This model was developed for an analogous effect in electrically conducting solutions in which the current flows through the solid elements of a network which cannot be penetrated by large charged particles.

We should add here that the multipath effect in packed beds might also perturb equilibrium and thus retention in the gel exclusion chromatography of large particles. The hydrodynamic effect described above would lead to concentrations higher than the equilibrium values near the fixed surfaces, and thus a higher-than-expected partitioning of particles into the pores at the surface.

The disturbances in retention suggested above would be most evident for reduced velocities, $\nu = d_p\langle v\rangle/D$, much greater than unity. Quantity d_p is the mean particle diameter of the fixed bed. Unfortunately, almost all liquid chromatography is run under conditions such that $\nu > 1$ (usually $\nu \gg 1$) as a practical matter (*19*).

Field-flow fractionation (FFF) is not subject to the severe complications of packed-bed hydrodynamic chromatography because its channel is always without obstructions. The channel geometry is uniform and mathematically tractable such that the theoretical predictions of mean displacement velocity under the influence of various applied fields has been highly successful.

The width, w, of FFF channels is typically 0.25 mm, or 250 μm. Clearly finite-size effects for ~ 1 μm particles unaffected by a field would be small. A lateral field or force, however, compresses the particle cloud near one wall, and its mean altitude, l, may be no more than a few μm. We regard 10 μm as typical, but considerably smaller values are sometimes realized. Under these circumstances, and with particles approaching 1 μm diameter, finite size effects are expected to have a significant role in retention and dispersion, much as outlined by the theory of this paper.

TABLE 1

Experimental Retention Volumes V_r of Polystyrene Latex Beads in Sedimentation FFF Compared to Theoretical Values (a) Allowing for Finite Particle Size ($R = 6\alpha + 6\lambda_{id}$) and (b) Totally Neglecting Particle Size ($R = 6\lambda_{id}$)

Particle diameter (μm)	Experimental V_r	V_r (ml) Theoretical (a) V_r	Theoretical (b) V_r
0.765	86.3	87.0	98.8
0.982	164	135	185

Previously published FFF data to test the foregoing theory are scarce because particle size effects have been minor in most work. We have recently completed an experiment with sedimentation FFF, however, that permits an initial test of retention theory (*25*). Polystyrene latex beads of diameters 0.982 and 0.765 μm were retained in a 5.21-ml volume column for 49 ml at 21 gravities, following which elution was completed at 11.8 gravities. The elution volume V_r was calculated as the sum of the two volumes corresponding to the respective field strengths by the equation

$$V_r = V_1 + V^0(1 - V_1R_1/V^0)/R_2 \tag{31}$$

where V_1 is the first component of the elution volume—49 ml in this case—and V^0 is the column volume—5.21 ml. Retention ratios R_1 and R_2 correspond to the two respective levels of field strength noted. We have calculated the necessary R_1 and R_2 values by using (a) Eq. (16), $R = 6\alpha + 6\lambda_{id}$, and (b) $R = 6\lambda_{id}$, the latter applicable when particle size is negligible, $\alpha \to 0$. The results are shown in Table 1.

Examination of the table shows that the particle size effect is quite accurately predicted with the 0.765 μm particles, but only partly accounted for with 0.982 μm particles. Since retention calculations in sedimentation FFF are generally quite accurate (*10*), the discrepancy cannot be quickly assigned to random errors or to distortions unrelated to particle size. Yet no particle-size effect can be identified from the limited data. It is possible that the larger particles are driven to the wall with sufficient force that some type of particle–wall interaction creates an additional retention effect. An evaluation of this hypothesis, unfortunately, must await the accumulation of additional experimental evidence.

Acknowledgments

The author would like to acknowledge computational assistance by

Dr. John Moellmer and Mr. Steven Giddings. Dr. Marcus N. Myers executed the calculations shown in Table 1. This investigation was supported by Public Healthe Service Research Grant GM 10851–20 from the National Institutes of Health.

REFERENCES

1. R. L. Whitmore, *Rheology of the Circulation*, Pergamon, Oxford, 1968.
2. E. A. DiMarzio and C. M. Guttman, *J. Polym. Sci.*, *B*, *7*, 267 (1969).
3. E. A. DiMarzio and C. M. Guttman, *Macromolecules*, *3*, 131 (1970).
4. C. M. Guttman and E. A. DiMarzio, *Ibid.*, *3*, 681 (1970).
5. H. Small, *J. Colloid Interface Sci.*, *48*, 147 (1974).
6. S. Mori, R. S. Poster, and J. F. Johnson, *Anal. Chem.*, *46*, 1599 (1974).
7. J. C. Giddings, *Sep. Sci.*, *1*, 123 (1966).
8. E. Grushka, K. D. Caldwell, M. N. Myers, and J. C. Giddings, in *Separation and Purification Methods*, Vol. 2 (E. S. Perry, C. J. Van Oss, and E. Grushka, eds.), Dekker, New York, 1974, p. 127.
9. M. N. Myers, K. D. Caldwell, and J. C. Giddings, *Sep. Sci.*, *9*, 47 (1974).
10. J. C. Giddings, F. J. F. Yang, and M. N. Myers, *Anal. Chem.*, *46*, 1917 (1974).
11. J. C. Giddings, F. J. F. Yang, and M. N. Myers, *Sep. Sci.*, *10*, 133 (1975).
12. J. C. Giddings, F. J. F. Yang, and M. N. Myers, *Science*, *193*, 1244 (1976).
13. J. C. Giddings, M. N. Myers, F. J. F. Yang, and L. K. Smith, in *Colloid and Interface Science*, Vol. 4, Academic, New York, 1976.
14. K. D. Caldwell, L. F. Kesner, M. N. Myers, and J. C. Giddings, *Science*, *176*, 296 (1972).
15. H. Brenner and L. J. Gaydos, *J. Colloid Interface Sci.*, *58*, 312 (1977).
16. J. C. Giddings, *J. Chem. Phys.*, *49*, 1 (1968).
17. J. C. Giddings, Y. H. Yoon, K. D. Caldwell, M. N. Myers, and M. E. Hovingh, *Sep. Sci.*, *10*, 447 (1975).
18. S. Krishnamurthy and R. S. Subramanian, *Ibid.*, *12*, 347 (1977).
19. J. C. Giddings, *Dynamics of Chromatography. Part I. Principles and Theory*, Dekker, New York, 1965.
20. J. C. Giddings, *Nature*, *184*, 357 (1959).
21. J. C. Giddings, *Anal. Chem.*, *35*, 1338 (1963).
22. H. Kaizuma, M. N. Myers, and J. C. Giddings, *J. Chromatogr. Sci.*, *8*, 630 (1970).
23. E. Grushka, L. R. Snyder, and J. H. Knox, *Ibid.*, *13*, 25 (1975).
24. J. C. Giddings and J. R. Boyack, *J. Theor. Biol.*, *2*, 1 (1962).
25. J. C. Giddings, F. J. Yang, and M. N. Myers, *J. Colloid Interface Sci.*,

Received by editor May 20, 1977